

# An Unusual Radio Galaxy in Abell 428: A Large, Powerful FR I Source In A Disk-Dominated Host

Michael J. Ledlow<sup>1,2</sup>  
New Mexico State University, Dept. of Astronomy  
Las Cruces, NM 88003

Frazer N. Owen<sup>1</sup>  
National Radio Astronomy Observatory<sup>3</sup>  
Socorro, NM 87801

and

William C. Keel<sup>1</sup>  
University of Alabama, Dept. of Physics and Astronomy  
Tuscaloosa, AL 35487

<sup>1</sup>Visiting Astronomer, Kitt Peak National Observatory, National Optical Astronomy Observatories, operated by the Association of Universities for Research in Astronomy, Inc., under contract with the National Science Foundation.

<sup>2</sup>Present Address: Institute for Astrophysics, University of New Mexico, Albuquerque, NM 87131

<sup>3</sup>The National Radio Astronomy Observatory is operated by Associated Universities, Inc., under contract with the National Science Foundation.

## ABSTRACT

We report the discovery of a powerful ( $\sim 10^{24} h_{75}^{-2} W Hz^{-1}$  at 20cm) FR I radio source in a highly flattened disk-dominated galaxy. Half of the radio flux from this source is concentrated within the host galaxy, with the remainder in a pair of nearly symmetrical lobes with total extent  $\sim 200$  kpc nearly perpendicular to the disk. The traditional wisdom maintains that powerful, extended radio sources are found only in ellipticals or recent merger events. We report B, R, J, and K imaging, optical spectroscopy, a rotation curve, an IRAS detection, and a VLA 20 cm image for this galaxy, 0313-192. The optical and near infrared images clearly show a disk. We detect apparent spiral arms in a deep B band exposure, and a dust-lane from a higher resolution B band image. The reddened nucleus is consistent with extinction by a similar dust-lane. The optical spectrum suggests a central AGN and some evidence of a starburst, with both the AGN and central starlight appearing substantially reddened (perhaps by the optical dust-lane). From analysis of the extended line emission in [OIII] and  $H\alpha$ , we derive a rotation curve consistent with an early-type, dusty spiral seen edge-on. From the IRAS detection at 60 and  $100\mu m$  we find that the ratio of Far IR to radio flux places this object firmly as a radio galaxy (i.e. the radio emission is not powered by star formation). The radio structure suggests that the radio source in this galaxy is related to the same physical mechanisms present in jet-fed powerful radio sources, and that such powerful, extended sources can (albeit extremely rarely) occur in a disk-dominated host.

## 1. Introduction and Background

Current wisdom on the nature of powerful, extended radio sources reflects the observation that whenever an unequivocal morphological classification is possible, the host galaxies are always ellipticals or recent merger remnants (Wilson & Colbert 1995, Urry & Padovani 1995, Antonucci 1993). This trend has driven several explanations for how the environment within the galaxy affects the large-scale radio structure. The difference between radio-loud and radio-quiet objects has recently been explained by Wilson & Colbert (1995) as connected to different host galaxy populations. The merger of two radio-quiet disk galaxies and the subsequent spin-up of a binary black hole produced in the merger event (assuming the individual holes are of approximately equal mass) would produce central objects of the greatest angular momentum uniquely in elliptical hosts or pre-elliptical mergers. Wholesale merging in clusters is implied by the high spiral fractions seen in galaxy clusters at high redshift as compared to the present epoch, as spirals and S0's merge to form ellipticals over cosmic time. Hutchings, Janson, & Neff (1989) and Smith *et al.* (1986) have argued that the host galaxies of radio-quiet quasars are spirals whereas the radio-loud quasars are found in elliptical hosts, consistent with the distinction in parent populations. However, HST imaging (*e.g.* Bahcall et al. 1996) has shown that reality is more complex; there exist unambiguous elliptical hosts of several radio-quiet QSOs, and probable spiral hosts for some radio-loud objects. The radio emission in many of these objects comes strictly from a small core rather than extensive double lobes, so it is not yet clear that the test is significant as regards to extensive double radio sources.

The standard picture of FR I and FR II radio sources (Fanaroff & Riley 1974) is that the extended structures in both classes are fueled by an active nucleus with outflows or jets that transport the radio plasma to large distances from the nucleus. For radio powers  $> 10^{23} h_{75}^{-2} W Hz^{-1}$  at 20cm, nearly all radio sources fit into one of the two FR categories and are hosted by elliptical galaxies (or recognizable variations on ellipticals) as found by Heckman et al. (1986) and Zirbel (1996, and references therein) for radio sources not selected to reside in rich cluster environments. In rich clusters the host galaxies appear to be much more homogeneous in nature, with a lower frequency of obvious merger activity (Ledlow & Owen 1995b).

Powerful starbursts and spirals are frequently observed with radio luminosities  $> 10^{22} h_{75}^{-2} W Hz^{-1}$ , but the origin of the radio emission seems to be very different from the FR jet-fed powerful radio galaxies. In both starbursts and luminous spirals (Hummel 1981, Condon *et al.* 1982), the radio emission is almost always limited to the nucleus and disk, and is dominated by either non-thermal emission from cosmic rays produced in supernovae or thermal emission from HII regions (both of which closely trace the distribution of star

formation). Radio surveys of Seyfert galaxies (Ulvestad & Wilson 1984a,b, 1989; Unger *et al.* 1986; Baum *et al.* 1993; Colbert *et al.* 1996a,b) which are nearly always identified with spiral/S0 hosts, indicate that the radio emission may arise from 3 components: (1) sub-kpc emission associated with the nucleus; jets are frequently detected, but with no preferred axis relative to the galaxy disk (Baum *et al.* 1993). (2) Extra-nuclear (kpc-scale) emission, and (3)  $>$  kpc-scale emission associated with the disk or spiral arms of the galaxy. The  $>$  kpc-scale emission is most often diffuse, resembling *bubbles*, with no indication for tightly collimated outflow (implied opening/cone angles are typically  $60^\circ$ ). The origin of the extra-nuclear emission is somewhat uncertain, although current models favor circumnuclear starbursts in which the cosmic ray electrons are *blown out* along the minor axis either trans/supersonically from pressure-driven winds (from either the starburst or an AGN) or subsonically in buoyant plumes (Baum *et al.* 1993). The correlation between the radio emission and starburst activity is additionally supported by the tight Far IR/Radio correlation observed in spiral galaxies and most Seyferts (Baum *et al.* 1993; Wilson *et al.* 1992; Rodriguez-Espinosa *et al.* 1987). To the contrary, powerful radio galaxies always show significantly more radio emission than predicted by the FIR/Radio correlation. In no case has extended radio emission been detected on  $>$  100 kpc scales in either luminous starburst or Seyfert galaxy samples. The largest scale outflows detected in Seyfert galaxy samples span tens of kiloparsecs with little evidence for collimated emission on these scales (Colbert *et al.* 1996a; Kukula *et al.* 1995). The radio emission in AGN spiral galaxies often resembles the features of classical radio galaxies, but at much lower radio powers and with sizes up to 2-3 orders of magnitude smaller in scale.

Additionally, the radio luminosity function of Seyferts, spirals, and radio galaxies are distinct and do not join one another, suggesting either differing parent populations or physical processes responsible for the radio emission (Meurs & Wilson 1984). It has been suggested that the parsec-scale jets which are seen in many Seyfert and spiral galaxies are smothered or disrupted by the dense surrounding gas and turbulent velocity field in the circumnuclear environment and are unable to escape to feed large-scale structures. It seems surprising, however, that the *jet-smothering* processes should be 100% efficient, but to date, there have been only a few observed  $>$ kpc-scale collimated outflows from spiral or S0 hosts (Wilson 1996), and no confirmed spiral or disk-dominated galaxy has ever been identified with extensive double-lobed FR I or FR II-like radio morphology (Véron & Véron-Cetty 1995).

The issue of whether spiral galaxies can ever host powerful FR I or II radio sources has a checkered history, exacerbated by morphological misclassifications and radio positions of insufficient accuracy. Shaver *et al.* (1983) investigated the spiral galaxy associated with the FR II source PKS 0400-181, and found that this is most probably a superposition

along the line of sight and that the radio source is located at  $z \sim 0.5$ . The properties of this system were recently confirmed as a superposition of a spiral at  $z=0.0367$  and a background elliptical at  $z=0.341$  (Rönnback & Shaver 1996). Identification issues also cloud the reported identifications of 3C 178 and 4CT 69.05.1 with nearby spirals. Further confusing the issue is the appearance of spiral-like features in emission lines in otherwise elliptical or S0 host galaxies, as in 3C 33 (Simkin & Michel 1986), 3C 305 (Heckman *et al.* 1985), PKS 1718-649 (Keel & Windhorst 1991), and IRAS 0421+040 (Beichman *et al.* 1985; Hill *et al.* 1988; Holloway *et al.* 1996) among others.

Where do S0 galaxies fit in the radio galaxy hierarchy? In one of the largest samples of S0's, Sadler *et al.* (1989) determined that the probability for radio emission was significantly lower than for ellipticals at the same total luminosity. However, if one considered the bulge component alone, the amplitude of the radio luminosity function for S0's and ellipticals was nearly identical at the same optical luminosity. In the radio S0's almost always resemble the structures seen in spiral galaxies (compact emission limited to the nucleus or disk of the galaxy).

Zirbel (1996) reported 6 possible S0? radio galaxy identifications from a large sample of very powerful radio galaxies ( $10^{26} < P_{408MHz} < 10^{28} h_{50}^{-2} W Hz^{-1}$ ). These candidate S0's were characterized by high central surface-brightness (a bright bulge component, typical of other D or cD galaxies in her sample) and an outer profile which fell more steeply than an average elliptical. However, none of the 6 objects classified as S0? exhibited spiral features or possessed a significant flattened disk component. Much of the ambiguity associated with these classifications results from the heterogeneous nature of the S0 class. We discuss this point further in section 4.

To date, only four historically classified disk-like galaxies have been claimed to exhibit FR-like radio morphology (collimated  $>kpc$  jets and lobes extending beyond the optical size of the host galaxy); 3C 305, 3C 293, NGC 5972, and NGC 0612. With the exception of NGC 5972 all of these objects are listed in a catalog of dusty ellipticals (Ebneter & Balick 1985). Both 3C 293 and 3C 305 are flattened ( $\epsilon \sim 0.4 - 0.5$ ) and possess a disk of rotating emission-line gas (Heckman *et al.* 1985). However, Heckman *et al.* found no evidence for a stellar disk in either system (stellar rotational velocities significantly less than the emission-line gas), and classified both objects as peculiar ellipticals. The radio source in 3C 305 is also quite small (a few kpc). From a sample of 347 nearby radio galaxies, NGC 5972 (classified as S0-a) was the only *disk* galaxy associated with a radio source significantly larger than the optical galaxy (500 kpc; Véron & Véron-Cetty 1995). Similarly, NGC 5972 possesses a rotating disk of high-ionization emission-line gas with no observable stellar disk, and was reclassified as an elliptical by the authors. NGC 0612 is

perhaps the most enigmatic of this group of objects. Ekers *et al.* (1978) noted that both a disk and nuclear bulge were quite distinct. The galaxy is bisected by a prominent dust-lane, somewhat similar in appearance to the Sombrero galaxy (M104) or Centaurus A. However, recent optical surface photometry of this system revealed that the outer profile (ignoring the prominent inner dust-lane) follows an  $r^{1/4}$ -law nearly perfectly (Fasano, Falomo, & Scarpa 1996). Consistent with the other objects in this group, Goss *et al.* (1980) measured extended, rotating emission-line gas out to 40 kpc from the nucleus. In all of these cases, a recent merger between an elliptical and a gas-rich disk-galaxy may be consistent with the observed properties and morphology, yet none of the four objects are dominated by a significant disk component. Thus to date there are no confirmed identifications of a large-scale, jet-fed radio source from a disk-dominated host, despite galaxy classifications as disk-like systems.

From our VLA 20cm survey of  $> 500$  Abell clusters (Ledlow & Owen 1995a; Owen, White, & Ge 1993; Owen, White, & Burns 1992), we have found one clearly disk-dominated galaxy with radio morphology resembling the powerful FR I radio sources. The survey was statistically complete to  $10^{23} h_{75}^{-2} W Hz^{-1}$  out to  $z=0.09$  though many sources were detected at lower redshifts with radio luminosities below this cutoff, including a number of spiral/S0 galaxies.

Abell 428 (Richness Class 0, Revised Rood-Sastry type C8, Bautz-Morgan type III) is very unusual in that nearly half of the galaxies within the inner 1 Mpc radius of Abell’s cluster position appear to be disk galaxies. Two radio sources were identified with this cluster, and cluster membership was confirmed from optical spectra (Owen, Ledlow, & Keel 1995). 0313-192 ( $z=0.067$ , the brighter of the two at  $S_{1400MHz} = 98$  mJy) is located 0.05 Abell radii or  $100h_{75}^{-1}$  kpc from Abell’s nominal cluster center. The total angular extent of its radio lobes is  $\sim 200h_{75}^{-1}$  kpc; nearly 100 times larger than the scale-height of the disk observed nearly edge-on! The other radio source (0314-192) is  $\sim 300h_{75}^{-1}$  kpc from the cluster center, is weaker (17 mJy), and is found in an elliptical host galaxy. R-band surface-photometry was reported for both sources in Ledlow & Owen (1995b).

In this paper, we present radio, optical, near-IR imaging, an IRAS detection, and optical spectroscopy of this galaxy. We examine the overall properties of the host galaxy to investigate possible peculiarities which might account for a disk galaxy showing such an unusual radio source. We present evidence which suggests that the radio emission in this galaxy is consistent with large-scale nuclear outflows driven by an imbedded AGN. From the combined analysis of the optical and near-IR imaging and optical spectroscopy, we argue that this galaxy is most consistent with an early-type spiral (Sa-Sb) classification. This appears to be the first detection of a powerful FR I radio galaxy with radio structure

greater than 100 kpc in size in an unambiguously disk-dominated host (whether S0 or genuine spiral). In section 2 we describe the observations. In section 3 we discuss the results from the radio, far IR, optical and near-IR imaging, and optical spectroscopy. We present our interpretation of the nature of this object and our conclusions in the discussion of section 4.

## 2. Observations

We have obtained followup optical imaging of 0313-192 in A428 at B-band using the KPNO 2.1m telescope on 1 January 1995. The KPNO *B* image is a 9-minute exposure obtained through thin cirrus with 1.0'' seeing using a 1024x1024 Tektronix CCD at a scale of 0.30 arcsec/pixel. We also observed 0313-192 in *B* using the Astrophysical Research Consortium's (ARC) 3.5m telescope at Apache Point Observatory (APO) on 13 October 1996. We obtained 13 10-min dithered exposures using a 2048x2048 Tek/SITe CCD. The chip was binned 2x2 on readout to produce a plate-scale of 0.28 arcsec/pixel. Conditions were non-photometric, and the seeing was moderate at  $\sim 1.3''$ . We observed A428 in the Cousins *R*-band using the KPNO 0.9m telescope on 11 August 1995 with the T2KA Tektronix 2048x2048 CCD. The *R* image has a total exposure time of 30 minutes with  $< 1''$  seeing during photometric conditions with a scale of 0.68 arcsec/pixel. For comparison, all these images were interpolated to a common grid with 0.3 arcsecond pixels. Magnitudes were transformed to the standard system from zero-point and extinction calibration from observations of Landolt (1992) equatorial standard stars.

The near-infrared *J* and *K* images were obtained at the ARC 3.5m telescope on 8 December 1995 using the GRIM II 256x256 NICMOS array in F/5 mode (0.48 arcsec/pixel). Seeing at *J* and *K* was 0.8 arcsec and sky conditions were photometric. Magnitudes were transformed to the standard system using observations of IR standard stars from Carter & Meadows (1995). At *J*, we obtained ten 60-second dithered exposures, alternating between source and sky. At *K*-band, we coadded 25 10-second exposures.

Following an initial blue spectrum for redshift measurement as part of a broader survey of radio sources in Abell clusters (Owen, Ledlow, & Keel 1995), we obtained an optical spectrum covering the broader range 3800–7400Å. This spectrum was obtained with the KPNO 2.1m telescope and GoldCam CCD spectrometer. To reduce problems with atmospheric dispersion at this southerly declination, 0313-192 was observed with the 2-arcsecond slit oriented north-south, which proved somewhat unfortunate since the disk is aligned nearly east-west. The exposure time was 20 minutes at a dispersion of 2.5 Å/pixel and resolution of  $\sim 6\text{Å}$ . Flux calibration used observations of the spectral standard star

Feige 54.

Additionally, we obtained a high-resolution spectrum of 0313-192 using the ARC 3.5m telescope on 12 October 1996. We used a 2" slit, rotating the instrument  $\approx 6^\circ$  to place the slit through the disk of the galaxy. We used the Double-Imaging Spectrograph (DIS), which separates the incoming beam blueward and redward of 5550Å using a dichroic filter. The detectors are a Tektronix 512x512 CCD on the blue-side, a TI 800x800 chip in the red. The plate-scales are 1.086 and 0.61 arcsec/pixel on the blue and red chips respectively. We used the highest resolution gratings (830.8 lines/mm in the blue and 1200 lines/mm in the red) with dispersions of 1.6 (blue) and 1.3 (Red) Å /pixel. The grating tilts were adjusted to center redshifted [OIII] $\lambda$ 5007, 4959 and  $H\beta$  on the blue chip, and  $H\alpha$ + [NII] in the red. We obtained 5 30-min exposures. The data were calibrated separately and coadded in two dimensions for analysis of possible extended line emission.

Radio observations were made at 1400 MHz with the VLA in both the B and C-arrays. The observations were made in snapshot mode (see Owen & Ledlow 1997) with typical integrations of 6 minutes. The data for each array were self-calibrated and combined in the UV-plane. We applied the primary-beam correction to the final map.

### 3. Results from Radio, Far-IR, Optical, and Near-IR Observations

#### 3.1. Radio Emission

Figure 1 shows an overlay of the 20cm radio emission (contours) onto the optical  $R$ -band image (grey-scale). Each of the radio lobes extend approximately 100 kpc in size; nearly two orders of magnitude larger than the scale-height of the disk seen nearly edge-on. Drawing a bisector from SW to NE through the radio lobes and galaxy nucleus we find an orientation PA=18° (north through east). The projected major axis of 0313-192 is oriented at PA $\sim 84^\circ$  on the  $R$ -band image, resulting in an inclination of the radio-lobe axis to the disk of 66° in the plane of the sky. In comparison with some other reported identifications of extended sources in spiral galaxies, we note that the optical and radio cores coincide to within 1". We can rule out a superposition with an elliptical cluster member of A428 given that we detect no trace of a halo surrounding 0313-192 down to very faint surface-brightness levels. If a superposition were responsible for our identification the host object would have to be at a much greater distance. The *a priori* probability of a chance superposition with a spiral galaxy with  $m_B \leq 17.5$  to within a coincidence of 1" is  $<0.1\%$  for our entire VLA survey of more than 500 clusters. (using the galaxy counts of Kirshner, Oemler, & Schechter 1979).



The integrated radio flux density from 0313-192 is  $\sim 98$  mJy. Nearly half of this (48 mJy) originates in the unresolved galaxy nucleus+disk. The northern radio lobe has an integrated flux density of 32 mJy, the southern lobe 18 mJy. Both radio lobes show indications of more diffuse emission out to larger distances, but deeper integrations will be necessary for a significant detection. With the radio image presented in this paper we do not detect actual *jet* emission (*i.e.* Bridle & Perley 1984). We have recently obtained followup higher resolution and higher frequency radio observations to look for evidence of collimated jet emission. We have confirmed the detection of a jet  $\approx 36$  kpc in length from the core extending into the southern lobe (Owen, Ledlow, & Keel 1997).

Based on the radio morphology, we classify 0313-192 as a powerful FR I radio galaxy. The morphology is very similar to the Fat-Double class defined in Owen & Laing (1989). The relationship between optical ( $M_{24.5}(R) = -21.26$ ) and radio luminosity ( $\log P_{20cm} = 23.95 W Hz^{-1}$ ) places 0313-192 very near the FR I/II break in the radio/optical luminosity plane (Ledlow & Owen 1996). The optical galaxy is one of the faintest in our survey, as no confirmed radio identifications out to  $z = 0.09$  were found with  $M_{24.5}(R)$  fainter than -21.

### 3.2. IRAS Far-Infrared Emission

We used the XSCANPI utility (to coadd individual IRAS scans) to estimate IRAS fluxes or upper limits for 0313-192 at 12, 25, 60, and  $100\mu m$ . At  $60\mu m$  we found a good detection with a flux density of  $110 \pm 23$  mJy. At  $100\mu m$  we measure a flux density of  $470 \pm 117$ . There was no detection at either 12 or  $25\mu m$ . Following Fullmer & Lonsdale (1989), we define the FIR flux as :

$$FIR = 1.26(2.58 \times 10^{12} f_{60} + 1.00 \times 10^{12} f_{100})10^{-26} W m^{-2} \quad (1)$$

where  $f_{60}$  and  $f_{100}$  are the IRAS flux-densities at 60 and  $100\mu m$ . Using the flux densities listed above, we find  $FIR = 9.50 \times 10^{-15} W m^{-2}$ .

The correlation between FIR and radio emission for spiral galaxies and Seyferts can be quantified via the parameter  $q$  (Helou *et al.* 1985) as

$$q = \log\left(\frac{FIR}{3.75 \times 10^{12} W m^{-2}}\right) - \log\left(\frac{S_\nu}{W m^{-2} Hz^{-1}}\right) \quad (2)$$

where  $S_\nu$  is the radio flux density. Using the total integrated radio emission from 0313-192 (98 mJy) we find  $q = 0.41$ . Using only the radio emission associated with the nucleus+disk (48.5 mJy), we find  $q = 0.72$ . Both values are considerably less than the canonical value of

$\langle q \rangle = 2.27 \pm 0.20$  at  $\nu = 1.45 \text{ GHz}$  for rich cluster spirals (Andersen & Owen 1995) or  $\langle q \rangle = 2.34 \pm 0.26$  from the entire IRAS bright galaxy sample (Condon 1991). Agreement with these  $q$ -values would require a FIR flux 35-75 times greater than is observed. In fact, many powerful radio galaxies (both elliptical and S0) have strong FIR emission (Golombek, Miley, & Neugebauer 1988). The excess radio emission over that predicted by the FIR/Radio correlation confirms our suggestion that this object be classified as a true radio galaxy, and provides no constraint as to the actual morphological type of this galaxy. Note that the spiral galaxy in the NW of the image in Figure 3 is only 39 arcsec ( $46h_{75}^{-1}$  kpc) in projected distance from 0313-192. Given the low resolution of the IRAS satellite, we cannot rule out that some fraction of the FIR flux arises from this source. Thus the values derived here should be viewed as strict upper limits.

### 3.3. Optical/Near-IR Imaging and Isophotal Surface Photometry

In Figure 2, we show grey-scale images of 0313-192 in  $B$ (KPNO),  $R$ ,  $J$ , &  $K$ . In Figure 3, we also show the deeper APO  $B$ -band image using two transfer functions; one to emphasize the blue properties of the galaxy disk, the other to examine the low surface brightness large-scale properties (down to 25.1 mag arcsec $^{-2}$  in the rest-frame of the galaxy). Inspection of the  $B$ -band images indicates several interesting features. (1) From the deep  $B$ -image, extending both east and west from the nucleus are features that we identify with a spiral arm. Although the disk is viewed nearly edge-on, the features clearly show an S-shaped symmetry about the nucleus. The arm emission is asymmetric, with the western arm somewhat brighter. (2) There is no evidence to suggest a tidal interaction with the galaxies to the SW or NW. There is an unusual feature at the west edge of the disk (an extension to the south), but this feature does not appear to have any connection to the neighboring galaxies. (3) From the shallower (but with better seeing)  $B$ -image in Figure 2, we see that the nucleus is diffuse, and the central brightness peak is bisected by a dark feature which we interpret as a dust-lane. The dust-lane has an apparent projected width of about 1 kpc (at the limit of our resolution). Dust lanes are not uncommon features in radio galaxies, even among those classified as ellipticals. De Koff *et al.* (1996) found that at least 30% of powerful 3C radio galaxies show indications of dust, either in clear dust-lanes or chaotically distributed throughout the galaxy. Thus, the presence of a dust-lane does not confirm a spiral classification for 0313-192. The spiral arm features present in the deep  $B$  image provide much more substantial evidence for such a classification. However, it is clear that the galaxy is strongly dominated by a flattened disk.

The nuclear continuum properties change strongly with wavelength. At  $B$ -band the

nucleus is very diffuse with no obvious image core. Moving to redder wavelengths, even at  $R$ , the nucleus and/or bulge contributes a substantial fraction of the galaxy light. At  $J$  and  $K$  the emission is strongly dominated by an unresolved core (or bulge at the limit of our resolution;  $1.1 \text{ h}_{75}^{-1} \text{ kpc}$ ). We are able to trace the disk out to  $\approx 20 \text{ kpc}$  in radius along the major-axis. Within a  $40 \text{ kpc}$  diameter aperture, we calculate absolute magnitudes of  $-19.9$ ,  $-21.4$ ,  $-23.1$ , and  $-24.4$  for  $B$ ,  $R$ ,  $J$ , and  $K$  respectively (corrected for galactic extinction).

We fit elliptical isophotes to each of the images using the method described in Jedrzejewski (1987). The centroid, ellipticity, and isophotal position-angle were allowed to vary at each radius. We show the major-axis surface-brightness, ellipticity, and position-angle profiles in Figure 4 for each color. The data points were binned in order to sample the seeing disk at two points per resolution element. The ellipticity profiles are reasonably consistent at all colors, with a strong trend for  $\epsilon$  to increase with radius up to a maximum  $\epsilon \sim 0.75$ . The outer optical isophotes are both highly elongated and “pointy”, indicating a highly inclined disk (since no true ellipticals have ellipticity greater than 0.7). There are small variations in position angle between the optical and near-IR bands, most likely related to the dust-lane or spiral features which are more prominent at the bluer colors.

In order to characterize the surface-brightness profiles for 0313-192, for the  $B$  and  $R$ -band images, we have fit a multi-component galaxy profile model of the form

$$I(r) = S_b \exp(-7.668 * [(\frac{r}{r_e})^{1/4} - 1]) + S_d \exp(-\frac{r}{r_0} + (\frac{r_1}{r})^3) \quad (3)$$

where  $S_b$  and  $S_d$  are the normalization scale factors for the bulge and disk components,  $r_e$  is the de Vaucouleurs effective (half-light) radius, and  $r_0$  is the radius of the exponential disk. In Figure 5, we show the result of the best-fit models. For purposes of these fits we have excluded points within the inner two seeing radii. We find  $r_e = 4.7, 1.9 \text{ kpc}$  and  $r_0 = 6.6, 5.8 \text{ kpc}$  for  $B$  and  $R$ -band respectively. The  $r_1$ -term was effectively zero. Neither profile is well-fit by a single-model (either  $r^{1/4}$  or exponential disk) over the entire range in radius. A pure disk model fits the profile quite well with the exception of the inner few kpc. A pure bulge/ $r^{1/4}$  model decays much too quickly to fit the profile beyond the inner several kpc. The larger  $r_e$  observed at  $B$ -band is consistent with the diffuse core as compared to the  $R$ -band image. For either value of  $r_e$  our resolution is sufficient to resolve the spheroidal component. Given the nature of the radio source, we expect that some fraction of the nuclear/spheroidal component arises from an unresolved core and AGN activity (as also evidenced by the very bright core at  $K$ -band). Thus, the bulge-to-disk ratio we measure should be viewed as an upper-limit, which most likely includes a non-thermal component from an imbedded AGN.

Following the method of Simien & de Vaucouleurs (1986), we have the calculated the

bulge-to-disk ratio for 0313-192 from the multicomponent fit. Defining  $k_1$  as the ratio of the integrated  $B$ -band luminosity of the spheroidal component to the total luminosity of the galaxy (both functions integrated to infinity), the bulge-to-disk ratio (B/D) is  $\gamma = k_1/(1 - k_1)$ . Simien & de Vaucouleurs examined the dependence of the magnitude difference between the bulge component and the total  $B$  magnitude ( $\Delta m = -2.5 \log(k_1)$ ) as a function of morphological type ( $T$ ). We find  $k_1 = 0.27$  and  $\gamma = 0.37$ . Using their interpolating functions for  $\Delta m(T)$ , we find  $T=2.6$ , consistent with a Hubble classification of Sa-Sb. As a comparison, S0 galaxies almost always have  $\gamma \geq 0.7$  (Dressler & Sandage 1983; Bothun & Gregg 1990), with most  $\geq 1$ . 0313-192 appears to fall in a region separate from S0's or lenticulars ( $T=-3-0$ ) and ellipticals ( $T<-3$ ).

Can we clearly rule out a S0 classification for 0313-192 based on the B/D ratio? There is significant scatter in the  $\Delta m(T)$  relation given by Simien & de Vaucouleurs, which they claim is due to photometric and decomposition errors with little contribution from classification errors or cosmic scatter (however, see Kennicutt 1981; Sandage 1961). In the mean, however, S0's clearly have larger B/D ratios. More importantly, S0's are usually defined as disk galaxies which have no recognizable spiral structure (Bothun & Gregg 1990). Given the appearance of what appear to be spiral arms and the low B/D ratio, we believe that the most consistent classification for 0313-192 is that of an early-type spiral (Sa-Sb).

### 3.4. Color Profiles

From the surface-brightness profiles at each color, we have calculated color profiles for  $B - R$ ,  $B - J$ ,  $B - K$ ,  $R - J$ ,  $R - K$ , and  $J - K$ . These profiles are shown in Figure 6. We have corrected the individual colors for galactic extinction, but have not applied a K-correction. Errors were determined from RMS deviations of the magnitude within each isophote. We have included a 5% calibration error for the near-IR bands, and a 2% uncertainty at  $B$  and  $R$ . The inner few kpc of the galaxy is highly reddened relative to the color of the disk. The nucleus is  $\approx 0.5-1$  magnitude redder than the disk depending on the particular color. In  $R - J$  and  $B - J$  the slope is much shallower from 2-4 kpc than in the other color profiles. At  $J$ -band, the core/bulge is much more prominent than at  $K$ , at which the galaxy is dominated by an unresolved core.

All of the derived nuclear colors strongly suggest the presence of significant amounts of dust, either associated with the nucleus itself or in the disk and associated dust-lane seen almost edge-on. Peletier & Balcells (1996) derived color profiles for 45 early-type spiral galaxies from the Uppsala catalog to study colors and color gradients in spiral bulges. Excluding those galaxies which they define as severely contaminated by dust, the average

nuclear  $B - R$  color is near 1.5 (we observe  $(B - R)_{nuc} \sim 1.9$ ). In addition, very few of their observed galaxies show strong gradients ( $>0.5$  mag) from this value at increasing radius in the disk. With the exception of the redder  $B - R$  color within the inner few kpc, 0313-192 is very similar to the objects in their sample. In near-IR colors, typical nuclear  $J - K$  values for ellipticals are  $\sim 1$ , for spiral galaxies  $J - K \sim 1 - 1.5$ , and nuclear starbursts have  $J - K$  in the range from 1-2 (Bothun 1991, Watson & Gallagher 1997). Watson & Gallagher show a few examples of nuclear starbursts with  $J - K \geq 2$ , although these are extreme cases. The nuclear  $J - K$  color observed in 0313-192 is more typical of some Seyfert 1 galaxies and Quasars (Ward *et al.* 1982; Hyland & Allen 1982), although a significant amount of dust ( $A_V > 5$ ) could shift a weak starburst/AGN or normal early-type spiral to our observed value. Additionally, our observed  $B - K$  nuclear color is strongly suggestive of dust (or a significant non-thermal K-band flux). Typical colors for spiral or S0 disks range from  $B - K = 3-4.3$  (Bothun & Gregg 1990). We observe a nuclear  $B - K$  color of  $\sim 6$  although the disk appears consistent with standard values. We discuss the possible interpretations of these results in the next section.

### 3.5. Nuclear Optical Spectra

In Figure 7, we show the KPNO optical spectrum for 0313-192. The y-axis is in units of  $F(\lambda)$  in  $ergs\ cm^{-2}\ sec^{-1}\ \text{\AA}^{-1}$ . The 2-d spectrum was convolved with a  $1''$  Gaussian along the spatial axis before extraction. We also convolved the spectrum with a  $5''$  Gaussian and extracted the spectrum separately. As the slit was oriented North-South, the spectrum should have very little contribution from the underlying disk of the galaxy.

The most prominent features in the spectrum are narrow emission from [OIII] $\lambda$ 5007, 4959,  $H\alpha + [NII]$ , [OI] $\lambda$ 6300, and weak [OII] $\lambda$ 3727,  $H\beta$ , and [SII] $\lambda$ 6716 + 6731. The narrow lines are suggestive of a Seyfert 2-like spectrum or possibly a powerful starburst.

From the calibrated spectrum we have calculated line and continuum ratios and equivalent widths (EW) for 0313-192. These values are listed in Table 1. Of particular interest is the very high  $H\alpha/H\beta$  ratio. We have corrected both  $H\alpha$  and  $H\beta$  for underlying stellar absorption, using the stellar absorption appropriate to old bulge populations (Keel 1983). These corrections are  $1.8\ \text{\AA}$  for  $H\alpha$  and  $1.3\ \text{\AA}$  at  $H\beta$  (the correction at  $H\beta$  is especially sensitive to any contribution from reddened hot stars). Consistent with the color profiles, such a high ratio is indicative of substantial dust. We do not detect any higher Balmer-line transitions in the spectrum. Another indication of the reddened core is in the  $4000\text{\AA}$  break (D4000). We find  $D(4000) = 2.15 \pm 0.18$ , which is consistent with the nominal value for elliptical galaxies, but much redder than expected for early-type spirals

or S0's (typical values are from 1.7-1.9; Kennicutt 1992). We measured all D(4000) values from the  $F(\nu)$ -calibrated spectrum. From the larger convolution (which includes more of the off-nuclear light) we find a bluer break ratio ( $1.96 \pm 0.14$ ) which may contain some contribution from the blue spiral-arms.

These line ratios are useful diagnostics of the relative importance of star-formation to a hard photoionizing continuum indicative of AGN activity and are relatively insensitive to internal extinction, as discussed by Baldwin, Phillips, & Terlevich (1981) and Veilleux & Osterbrock (1987). These values place 0313-192 as an intermediate case between AGN and powerful starburst activity. The [O I] strength is perhaps the strongest diagnostic, since star-forming nuclei are not observed with [O I]/ $H\alpha$  as high as the 0.1 we find. Based on the [OIII]/[OII]/[OI] ratios and fairly weak  $H\alpha$  (which is an indicator of massive star formation in addition to whatever nonstellar ionization is taking place), we suggest that the nuclear emission is dominated by weak AGN activity rather than a circumnuclear starburst. The substantial reddening implied by the broadband colors and Balmer decrement might make the nucleus intrinsically luminous, but seen from an unfavorable direction.

### 3.6. Extended Line Emission and Rotation Curve

While the core spectrum is useful in illuminating the AGN or nuclear starburst properties, off-nuclear spectra are required to search for evidence of a stellar disk. The primary diagnostics here are the  $H\alpha$  equivalent width, the  $H\alpha$ /[NII] ratio, and the Tully-Fisher relation. While there is some overlap along the Hubble sequence in these properties and S0's typically exhibit much more scatter than spirals, we can use these diagnostics to estimate the probable morphological classification. The largest uncertainty in these measurements is the unknown intrinsic extinction within the galaxy. Line-ratios are less sensitive to extinction.

From the high-resolution APO spectra centered on [OIII] and  $H\alpha$ + [NII], we find the emission to be highly extended throughout the disk. In Figure 8, we show rotation curves measured from these lines. It is interesting to note that the gas distribution appears asymmetric, as we trace extended line emission out to 15 kpc west of the nucleus and only  $\approx 10$  kpc to the east. This asymmetry is apparent in the  $B$ -band image of Figure 3, as the feature which we interpret as a spiral arm is significantly fainter to the east. The rotation curves are consistent with an edge-on dusty disk, with apparent solid-body rotation from the outer arms. There is some indication that the rotation curve begins to level-off at  $\approx 10$  kpc in radius. We find good agreement between the [OIII] and  $H\alpha$  velocities, although the [OIII] luminosity clearly diminishes more rapidly with increasing radius (is more confined

to the nuclear region). The [NII]/H $\alpha$  ratio in the disk is consistent with star formation ([NII] much weaker than H $\alpha$ ) and HII-region like spectra. We adopt a maximum rotational velocity of  $v_{rot}=208$  km sec $^{-1}$ .

### 3.7. The B-Band Tully-Fisher Relation

Fouqué et al. (1990) used a sample of 178 spiral galaxies in the Virgo cluster to determine the distance to the Virgo cluster against a calibrated B-band Tully-Fisher (TF) relation for 18 calibrator sources (with independent distance measurements.). Following their method, we determine  $B_T^C$  for 0313-192 measured to the 25 mag arcsec $^{-2}$  isophote in the rest-frame of the galaxy (includes a correction for galactic extinction and  $(1+z)^4$  surface-brightness diminution term). The largest uncertainty arises from the correction for internal extinction. We estimate the inclination from the classical formula (Hubble 1926):

$$\cos^2 i = \frac{q^2 - q_0^2}{1 - q_0^2} \quad (4)$$

where  $q$  is the observed axis ratio ( $\frac{b}{a} = 1 - \epsilon$ ) measured at the 25 mag arcsec $^{-2}$  isophote and  $q_0$  is the intrinsic axis ratio. We estimate  $q_0$  from the morphological type (T=2.6, from the bulge-to-disk ratio) using the fit given in Fouqué et al. We find  $q = q_0 = 0.27$  consistent with  $i \sim 90^\circ$  (within an error of order  $5^\circ$ ). For inclinations  $> 80^\circ$ , Fouqué et al. assume an internal extinction of 0.96 mags. Following a similar prescription, we find  $B_T^C = -20.79$  (Fouqué et al. use  $H_0 = 68$ ) compared to -20.76 predicted by the calibrated B-band TF relation. Such strong agreement with the prediction suggests that 0313-192 is indeed rotationally supported. Compared to the quartile ranges in the TF relation for the different spiral types, 0313-192 falls cleanly within the Sa-Sb range, consistent with our previous classification. Note, however, that there are claims that morphological segregation in the TF relation is an artifact of selection biases (Bottinelli *et al.* 1986; Fouqué *et al.* 1990).

Does the very good agreement with the TF relation rule out an S0 classification for 0313-192? Dressler & Sandage (1983) examined rotation curves for  $\approx 30$  field S0's. Plotted on the TF relation S0's span the entire range of all spiral types. Dressler & Sandage offer several possible explanations for the observed scatter. They concluded that variations in the M/L ratio and/or significant kinetic energy in velocity dispersion (pressure support) between different galaxies may explain the scatter. S0's are thus a very heterogeneous class. The distinction between an S0 or early-type spiral on the TF relation varies significantly from object to object. The very good agreement for 0313-192 with the TF prediction

is strongly suggestive of an early-spiral classification, however we can not rule out a coincidental result.

### 3.8. $H\alpha$ Line Strength and Line Ratios

From the  $H\alpha$  luminosity and equivalent width we compare 0313-192 to samples of early to late-type spirals and S0's. The EW measures listed in Table 1 correspond to nuclear values with little contribution from the disk. We use our high-resolution spectrum to measure the  $H\alpha$  luminosity for disk and nuclear components separately. After correcting the  $H\alpha$  equivalent widths for underlying stellar absorption ( $1.8\text{\AA}$  see previous section), we find the following values: integrated along slit (includes nucleus)  $EW=11.4\text{\AA}$ , pure disk (average of E and W components)  $EW=12.4\text{\AA}$ . We found  $EW=9.6\text{\AA}$  from the nuclear spectrum in Figure 7. Additionally, the disk has an emission spectrum consistent with HII regions ( $[\text{NII}]$  much weaker than  $H\alpha$ ) whereas the ionization parameter and line ratios in the nucleus are intermediate between a starburst and weak AGN activity. We have not corrected the  $H\alpha$  fluxes for internal extinction.

Kennicutt (1992) gives values for integrated  $H\alpha$  EW for early Hubble-type spirals (omitting nuclear starbursts and AGN) and found  $S_a=3$ ,  $S_b=4.5$ ,  $S_b=18$ , and  $S_{bc}=31\text{\AA}$ . No corrections were made for internal extinction. Based on these values, 0313-192 is placed firmly in the  $S_b$ - $S_b$  range. For S0's, Pogge & Eskridge (PE) (1993) observed 32 S0 galaxies selected by high  $HI$  mass and chosen to be nearly face-on. Both of these would enhance the observed equivalent widths as compared to a more random sample, and likely as compared to 0313-192 as well. This sample therefore represents the upper envelope of star formation in S0 galaxies. 14/32 of the objects were detected in  $H\alpha$ , with a large range in EW measures; they find the median  $H\alpha$   $EW=5.6 \pm 2.4$  (median  $L(H\alpha)=2.51 \times 10^{40}$  ergs  $\text{sec}^{-1}$ ). The difference in the median  $L(H\alpha)$  between the  $HI$ -rich S0 sample and 125 early to late-type spiral galaxies from Kennicutt & Kent (1983) (median  $L(H\alpha)=7.41 \times 10^{40}$  ergs  $\text{sec}^{-1}$ ) was statistically significant at the  $>99\%$  level. In comparison, we find an integrated  $L(H\alpha)=8.38 \times 10^{40}$  ergs  $\text{sec}^{-1}$  for 0313-192. Only 3/32 (9%) of the S0's in the PE sample have integrated  $H\alpha$  luminosities as high as 0313-192, and two of these objects are classified as nuclear starbursts. If we eliminate the two nuclear starburst galaxies, that leaves only 1/32 (3%) S0's with comparable  $H\alpha$  emission. Statistically, 0313-192 is much more consistent with an early-type spiral classification.



#### 4. Discussion and Conclusions

The optical morphology of 0313-192 is quite unusual for a source of this kind, with several indications that this is a spiral (and certainly a disk galaxy) rather than the normal elliptical. The radio power and morphology of 0313-192 are typical of a large, luminous FR I source, with the usual double-lobe structure and significant core emission. The radio lobes extend  $\approx 100$  kpc north and south of the disk. The nucleus is highly reddened, presumably from significant amounts of dust consistent with the observed dust-lane bisecting the nucleus in the disk seen nearly edge-on. The nuclear optical and IR colors are consistent with either a highly reddened ( $A_V > 5$  mag) core in a normal/starbursting spiral or from a (possibly non-thermal) quasar-like nucleus. The very bright, dominant core at K-band supports a possible non-thermal component, or an intrinsically luminous core which is mostly obscured at shorter wavelengths. The nuclear optical emission-line spectrum is intermediate between a starburst and weak AGN activity. In particular, the  $[\text{OI}]/H\alpha$  ratio (0.1) is significantly higher than found in circumnuclear starbursts. The near-IR color and weakness of FIR emission all argue in favor of an obscured AGN as the dominant energy source. We also find no evidence for a galaxy merger or interactions between 0313-192 and the neighboring galaxies to the NW and SW. This point is in stark contrast to the peculiar nature of all previous radio galaxy candidates discussed in the introduction.

While all diagnostics point towards an early spiral type (Sa-Sb), we cannot rule out an S0 classification given the large scatter and inhomogeneity of this class. Despite best efforts to bin galaxies into morphological classes which represent a physically meaningful stage of evolution or a homogeneity of properties, the true definition of an S0 remains somewhat mysterious. van den Bergh (1990) argues that “the S0 classification type comprises a number of physically quite distinct types of objects that exhibit only superficial morphological similarities.” This observation is consistent with the large scatter in fundamental properties such as the TF relation, central velocity dispersion, B/D ratio, the amount of gas and dust, and the degree of flattening. Thus, on an individual object basis, S0’s may have arrived at their present morphology via very different evolutionary paths (van den Bergh 1997). Additional confusion arises from the multitude of different classification schemes. A particularly good example is the galaxy IC 310 in the Perseus cluster. In the de Vaucouleurs (1959) classification scheme this galaxy was classified as SA(r)0, ( $r$  meaning ring-like structure), an S0 in the Hubble/Sandage system, and a D galaxy in the Morgan (1962) form-family based on its extended halo. Yet by all appearances IC 310 is a very round  $L^*$ -like elliptical ( $\epsilon \sim 0.05$ ) with very faint, possibly shell-like features at large radii. Such faint peculiar features are not uncommon in powerful radio galaxies, and it is precisely these features (tidal tails, fans, shells, bridges) which support the contention that galaxy mergers may be important in stimulating nuclear activity (Heckman *et al.* 1986). Nearly

all of the well-studied radio-loud *S0*'s are consistent with an elliptical-like host which has undergone a merger event with a disk galaxy thus producing a weak disk-component with significant dust.

Would an S0 classification diminish the apparent uniqueness of this object? We think not given that, regardless of the morphological classification, to the best of our knowledge no galaxy with the clearly disk-dominated features and apparent spiral structure of 0313-192 has ever been identified with a radio source of such large extent. As nearly half of the radio luminosity from this source arises in the lobes  $\approx 100$  kpc from the nuclear source, the origin of the radio emission is without question an AGN-driven, large-scale nuclear outflow rather than radio emission powered by star formation. In all respects, 0313-192 is consistent with the standard picture of powerful FR I radio galaxies, with the exception of its unusual optical morphology. To the best of our knowledge, this is the first reported detection of a large-scale FR I radio source in an unambiguously disk-dominated host galaxy.

### Acknowledgements

M.J.L. thanks Nick Devereux and Alan Watson for helpful discussions on the FIR and NIR properties of spiral galaxies. We thank Greg Bothun for his comments on an earlier draft of this paper. This work was partially supported by NSF Grant AST-9317596 to J.O. Burns and C. Loken. This research has made use of the NASA/IPAC Extragalactic database (NED) which is operated by the Jet Propulsion Laboratory, Caltech, under contract with the National Aeronautics and Space Administration.

### REFERENCES

- Andersen, V. & Owen, F.N. 1995, *AJ*, 109, 1582
- Antonucci, R.R.J., 1993, *ARA&A*, 31, 473
- Bahcall, J.N., Kirhakos, S., & Schneider, D.P. 1996, *ApJ*, 457, 557
- Baldwin, J.A., Phillips, M.M., & Terlevich, R. 1981, *PASP*, 93, 5
- Baum, S.A., O'Dea, C.P., Dallacassa, D., de Bruyn, A.G., & Pedlar, A. 1993, *ApJ*, 419, 553
- Beichman, C., Lonsdale, C.J., Wynn-Williams, C.G., Heasley, J.N., Becklin, E.E., Persson, S.E., Miley, G.K., Soifer, B.T., Neugebauer, G., & Houck, J.R. 1985, *ApJ*, 293, 148
- Bothun, G.D. & Gregg, M.D. 1990, *ApJ*, 350, 73
- Bothun, G. 1991, in *Astrophysics with Infrared Arrays*, ed. R. Elston (PASP, San Francisco), ASP Conf. Ser. 14, p. 19

- Bottinelli, L., Gouguenheim, L., Paturel, G., & Teerikorpi, P. 1986, *A&A*, 166, 393
- Bridle, A. & Perley, R. *ARA&A*, 22, 319
- Carter, B.S. & Meadows, V.S. 1995, *MNRAS*, 276, 734
- Colbert, E.J.M, Baum, S.A., Gallimore, J.F., O’Dea, C.P., Lehnert, M.D., Tsvetanov, Z.I., Mulchaey, J.S., & Caganoff, S. 1996a, *ApJS*, 105, 75
- Colbert, E.J.M, Baum, S.A., Gallimore, J.F., O’Dea, C.P., & Christensen, J.A. 1996b, *ApJ*, 467, 551
- Condon, J.J., Condon, M.A., Gisler, G., & Puschell, J.J. 1982, *ApJ*, 252, 102
- Condon, J.J. 1991, in *The Interpretation of Modern Synthesis Observations of Spiral Galaxies*, ASP Conf. Ser. (San Francisco), (N. Duric & P. Crane, eds.), Vol 18, p. 113
- De Koff, S., Baum, S.A., Sparks, W.B., Biretta, J., Golombek, D., Macchetto, F., McCarthy, P., & Miley, G. 1996, *ApJS*, 107, 621
- de Vaucouleurs, G. 1959, *Handb. der Physik*, 53, 311
- Dressler, A. & Sandage, A. 1983, *ApJ*, 265, 664
- Ebner, K & Balick, B. 1985, *AJ*, 183
- Ekers, R.D., Goss, W.M., Kotanyi, C.G., & Skellern, D.J., 1978, *A&A*, 69, L21
- Fanaroff, B.L. & Riley, J.M. 1974, *MNRAS*, 167, 31p
- Fasano, G., Falomo, R., & Scarpa, R. 1996, *MNRAS*, 282, 40
- Fouqué, P., Bottinelli, L., Gouguenheim, L., & Paturel, G. 1990, *ApJ*, 349, 1
- Fullmer, L., & Lonsdale, C. 1989, *Catalogued Galaxies and Quasars Observed in the IRAS Survey (NASA)*
- Golombek, D., Miley, G., & Neugebauer, G. 1988, *AJ*, 95, 26
- Goss, W.M., Danziger, I.J., Fosbury, R.A.E., & Boksenberg, A. 1980, *MNRAS*, 190, 23P
- Heckman, T.M., Illingworth, G.D., Miley, G.K., & van Breugel, W.J.M 1985, *ApJ*, 299, 41
- Heckman, T.M., Smith, E.P., Baum, S.A., van Breugel, W.J.M., Miley, G.K., Illingworth, G.D., Bothun, G.D., & Balick, B. 1986, *ApJ*, 311, 526
- Helou, G., Soifer, B.T., & Rowan-Robinson, M. 1985, *ApJ*, 298, 7
- Hill, G.J., Wynn-Williams, C.G., Becklin, E.E., & MacKenty, J.W. 1988, *ApJ*, 335, 93
- Holloway, A.J., Steffen, W., Pedlar, A., Axon, D.J., Dyson, J.E., Meaburn, J., & Tadhunter, C.N. 1996, *MNRAS*, 279, 171

- Hubble, E. 1926, ApJ, 64, 321
- Hummel, E. 1981, A&A, 93, 93
- Hutchings, J.B., Janson, T., & Neff, S.G. 1989, ApJ, 342, 660
- Hyland, A.R. & Allen, D.A. 1982, MNRAS, 199, 943
- Jedrzejewski, R.I. 1987, MNRAS, 226, 747
- Keel, W.C. 1983, ApJ, 269, 466
- Keel, W.C. & Windhorst, R.A. 1991, ApJ, 383, 135
- Kennicutt, R.C. 1981, AJ, 86, 1487
- Kennicutt, R.C. & Kent, S.M. 1983, AJ, 88, 1094
- Kennicutt, R.C. 1992, ApJ, 388, 310
- Kirshner, R., Oemler, G., & Schechter, P. 1979, AJ, 84, 951
- Kukula, M.J., Pedlar, A., Baum, S.A., & O’Dea, C.P. 1995, MNRAS, 276, 1262
- Landolt, A.U. 1992, AJ, 104, 340
- Ledlow, M. J. & Owen, F. N. 1995a, AJ, 109, 853
- Ledlow, M.J. & Owen, F.N. 1995b, AJ, 110, 1959
- Ledlow, M.J. & Owen, F.N. 1996, AJ, 112, 9
- Meurs, E.J.A. & Wilson, A.S. 1984, A&A, 136, 206
- Morgan, W.W. 1962, ApJ, 135, 1
- Owen, F.N. & Ledlow, M.J. 1997, ApJS, 108, 41
- Owen, F.N., White, R.A., & Burns, J.O. 1992, ApJS, 80, 501
- Owen, F.N., White, R.A., & Ge, J.-P. 1993, ApJS, 87, 135
- Owen, F.N., Ledlow, M.J., & Keel, W.C. 1995, AJ, 109, 14
- Owen, F.N., Ledlow, M.J., & Keel, W.C. 1997, in preparation
- Owen, F.N. & Laing, R.A. 1989, MNRAS, 238, 357
- Peletier, R.F. & Balcells, M. 1996, AJ, 111, 2238
- Pogge, R.W. & Eskridge, P.B. 1993, AJ, 106, 1405
- Rodriguez-Espinoza, J.M., Rudy, R.J., & Jones, B. 1987, ApJ, 312, 555
- Rönnback, J. & Shaver, P. 1996, preprint
- Sadler, E.M., Jenkins, C.R., & Kotanyi, C.G. 1989, MNRAS, 240, 591

- Sandage, A. 1961, *the Hubble Atlas of Galaxies*, Carnegie Institute of Washington Pub. No. 618
- Simien, F. & de Vaucouleurs, G. 1986, ApJ, 302, 564
- Shaver, P.A. *et al.* 1983, MNRAS, 205, 819
- Simkin, S.M. & Michel, A. 1986, ApJ, 300, L5
- Smith, E.P., Heckman, T.M., Bothun, G.D., Romanishin, W.R., & Balick, B. 1986, ApJ, 306, 64
- Ulvestad, J.S. & Wilson, A.S. 1984a, ApJ, 278, 544
- Ulvestad, J.S. & Wilson, A.S. 1984b, ApJ, 285, 439
- Ulvestad, J.S. & Wilson, A.S. 1989, ApJ, 343, 659
- Unger, S.W., Pedlar, A., Booler, R.V., & Harrison, B.A. 1986, MNRAS, 219, 387
- Urry, C.M. & Padovani, P. 1995, PASP, 107, 803
- van den Bergh, S. 1990, ApJ, 348, 57
- van den Bergh, S. 1997, AJ, 113, 2054
- Veilleux, S. & Osterbrock, D.E. 1987, ApJS, 63, 295
- Véron, P. & Véron-Cetty, M.-P. 1995, A&A, 296, 315
- Ward, M., Allen, D.A., Wilson, A.S., Smith, M.G., & Wright, A.E. 1982, MNRAS, 199, 953
- Watson, A.M. & Gallagher, J.S. 1997, in preparation
- Wilson, A.S. 1996, in *Energy Transport in Radio Galaxies and Quasars*, eds. P. Hardee, A. Bridle, & A. Zensus (PASP, San Francisco), ASP Conf. Ser. 100, p. 9
- Wilson, A.S. & Colbert, E.J.M. 1995, ApJ, 438, 62
- Wilson, A.S., Elvis, M., Lawrence, A., & Bland-Hawthorn, J. 1992, ApJ, 391, L75
- Zirbel, E. 1996, ApJ, 473, 713

Table 1. Nuclear Emission-Line Strengths and Line/Continuum Ratios

Feature	Flux $ergs\ cm^{-2}\ s^{-1}$	EW $\text{\AA}$	Ratio
$H\alpha$	7.7e-15	9.6	...
[NII] $\lambda$ 6586	1.3e-15	2.0	...
$H\beta$	2.2e-15	2.8	...
[OIII] $\lambda$ 5007	1.8e-14	19.6	...
[OII] $\lambda$ 3727	9.7e-16	3.3	...
[OI] $\lambda$ 6300	6.9e-16	0.6	...
[SII] $\lambda$ 6716 + 6731	1.2e-15	0.5	...
[OIII]/ $H\beta$	...	...	7.9
[NII]/ $H\alpha$	...	...	0.2
$H\alpha/H\beta$	...	...	3.5
[OIII]/[OII]	...	...	18.2
[OIII]/[OI]	...	...	25.6
[OI]/ $H\alpha$	...	...	0.1
[SII]/ $H\alpha$	...	...	0.2
$D(4000)_1''$	...	...	$2.15 \pm 0.18$
$D(4000)_3''$	...	...	$1.96 \pm 0.14$

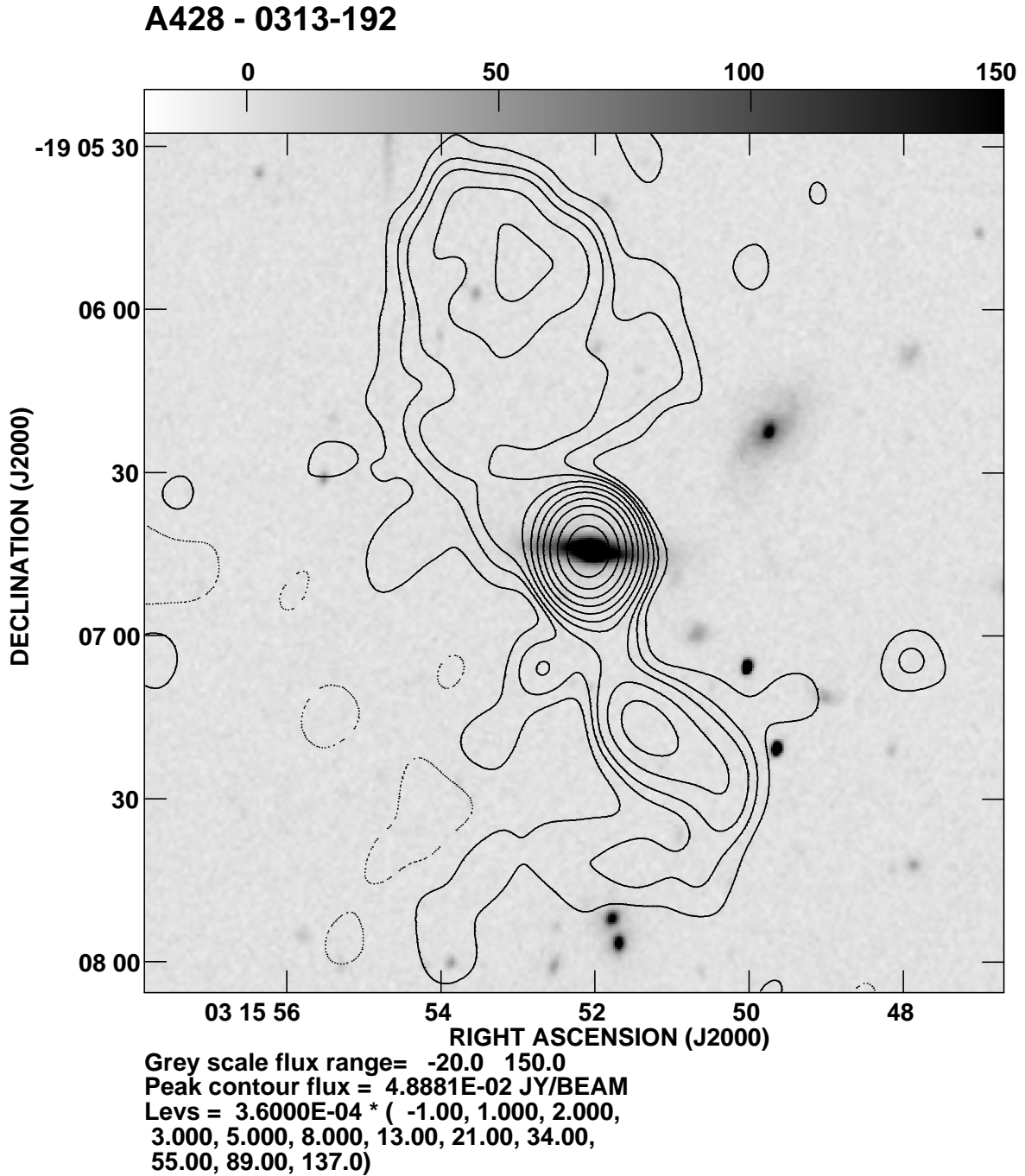


Fig. 1.— Radio (20cm)/Optical (R-band) overlay for 0313-192. The radio source extends  $\approx$  100 kpc north and south of the host galaxy.

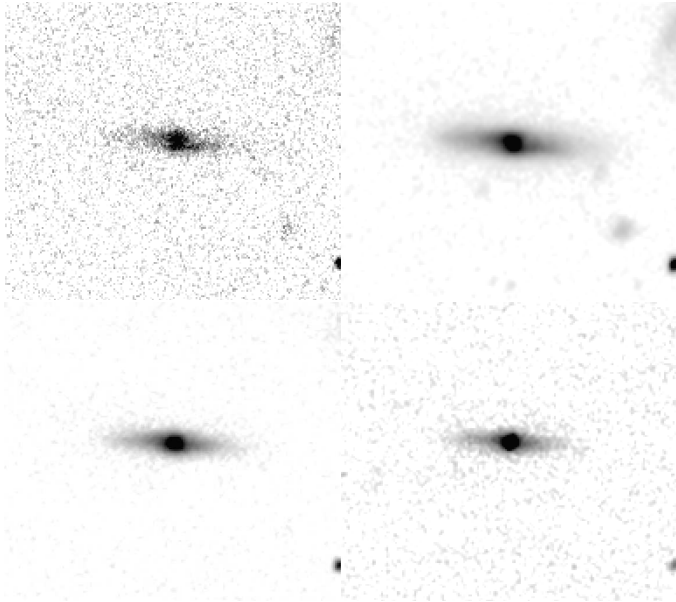


Fig. 2.— Grey-scale images at B, R, J, and K. We have applied a transfer function scaled by the square-root. Upper left=B (KPNO), upper right=R, lower left=J, lower right=K.



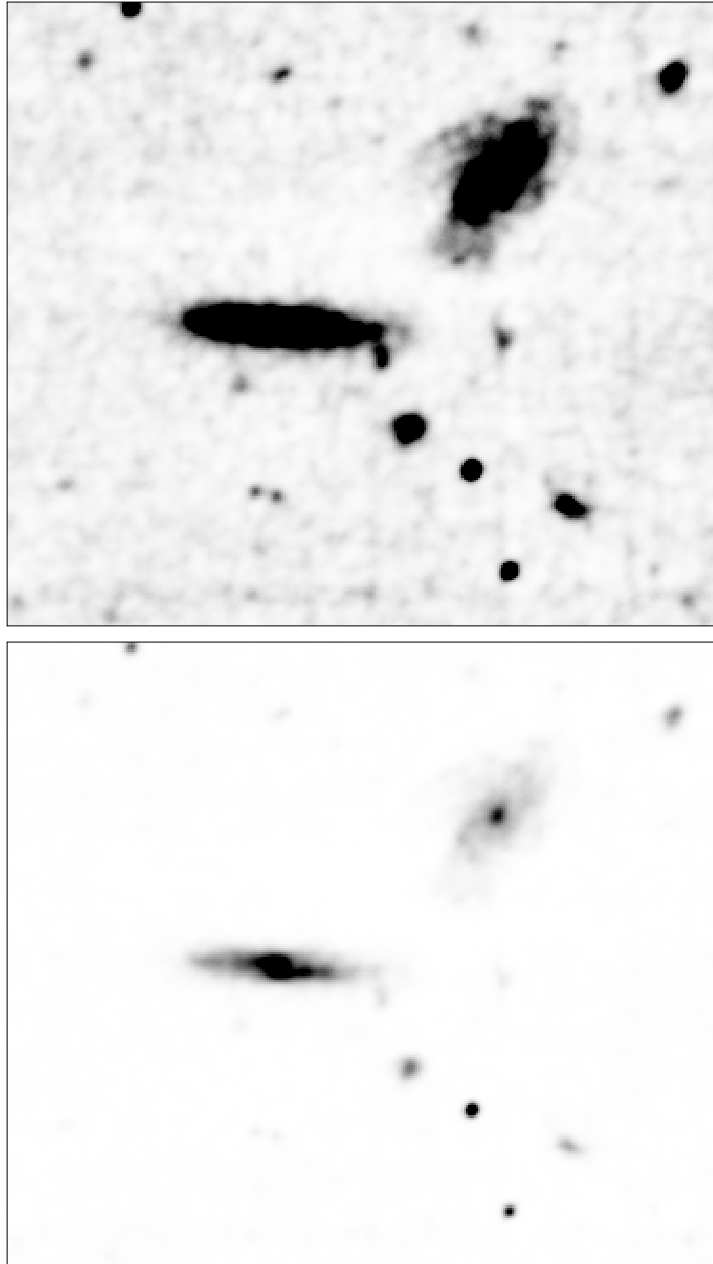


Fig. 3.— A deep B-band grey-scale image from the ARC 3.5m telescope. Top: transfer function chosen to accentuate low surface-brightness features and to look for evidence of an interaction with the neighboring galaxies. Bottom: transfer function chosen to bring out the features in the disk.

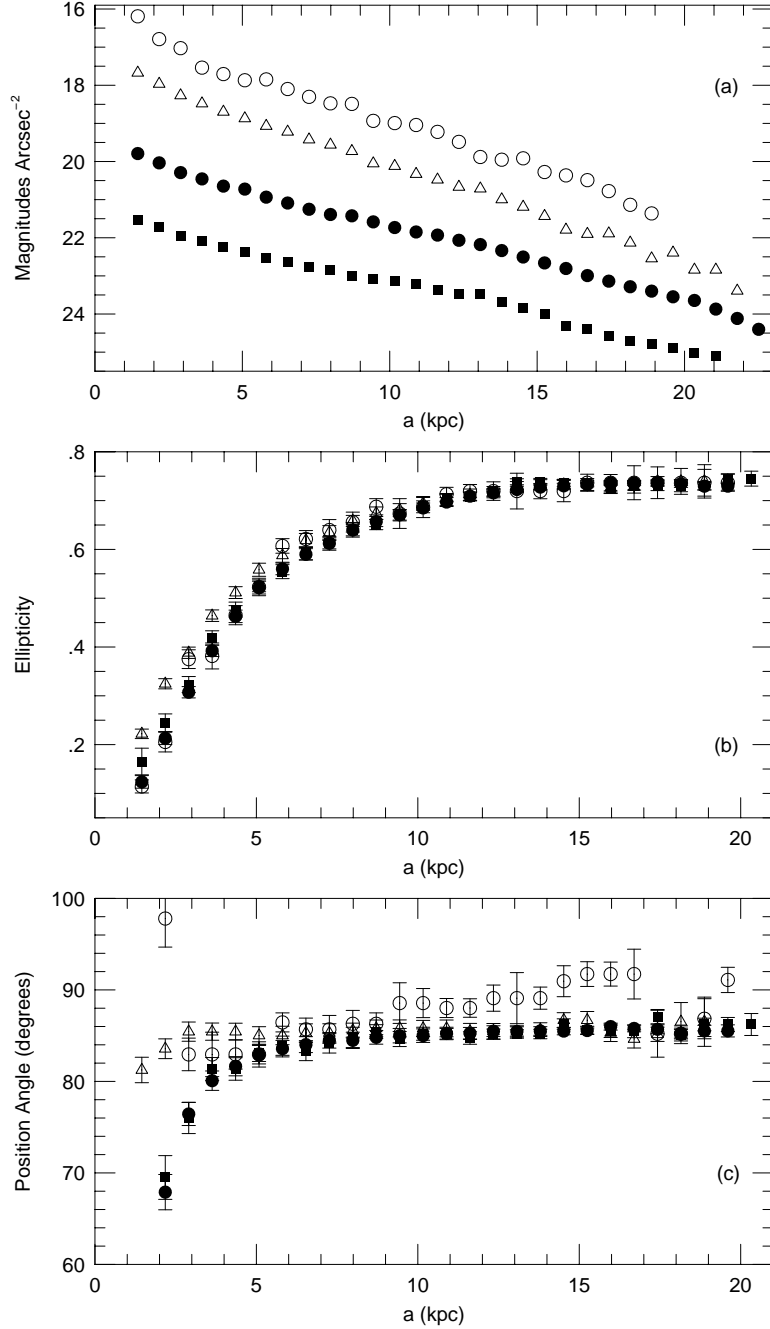


Fig. 4.— Results of isophotal fitting at B (filled squares), R (filled circles), J (open triangles), and K (open circles). (a) The surface-brightness profiles for each color. The surface brightness is corrected to the rest-frame of the galaxy. (b) The ellipticity profiles as a function of radius at each color. (c) The variation in position angle with color.

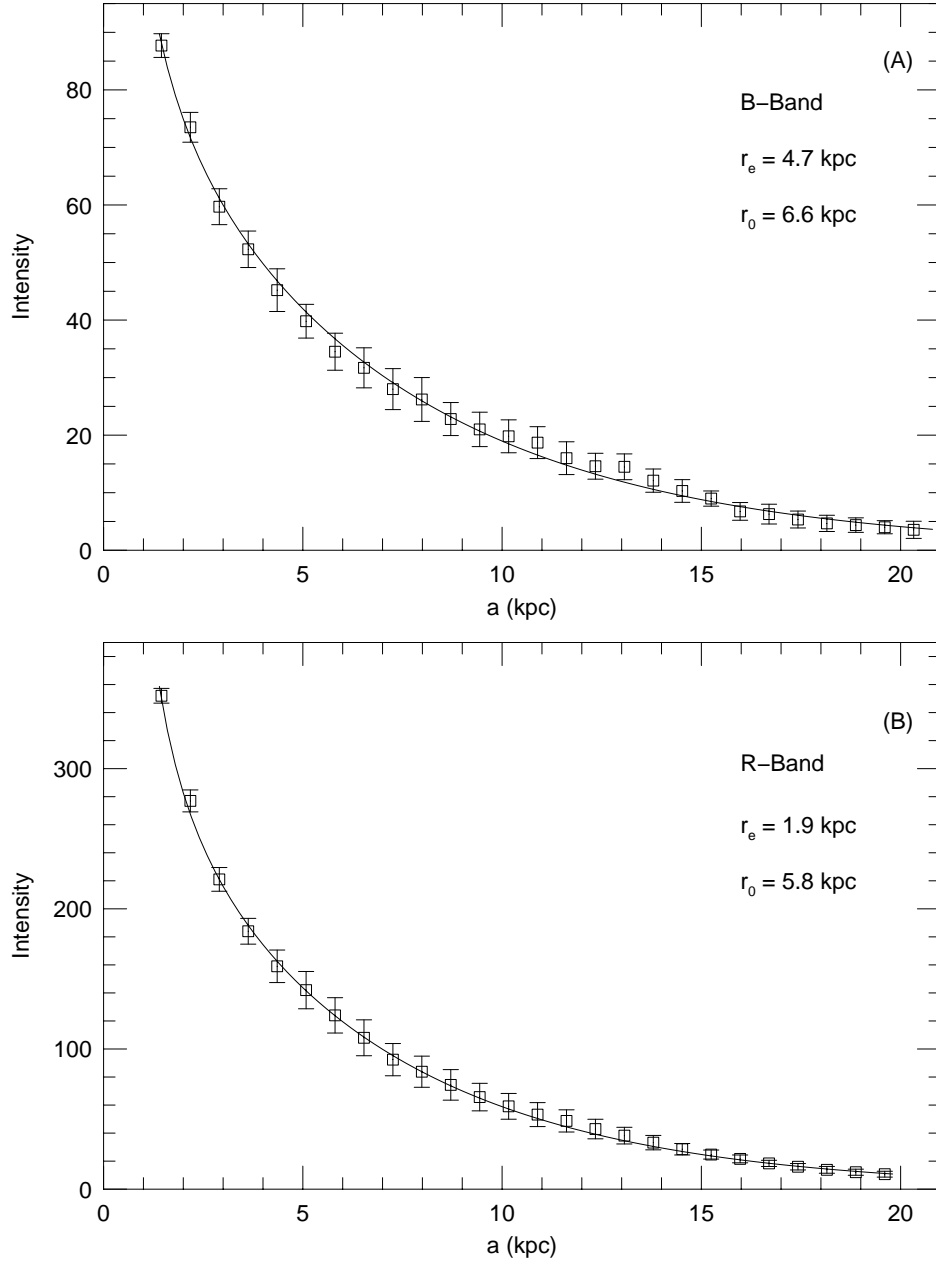


Fig. 5.— The decomposition of the major-axis intensity profile into bulge and disk components. The solid-line is the best-fit combined bulge+disk model. The fit parameters are labeled on the plot. (a) B-band, (b) R-band.

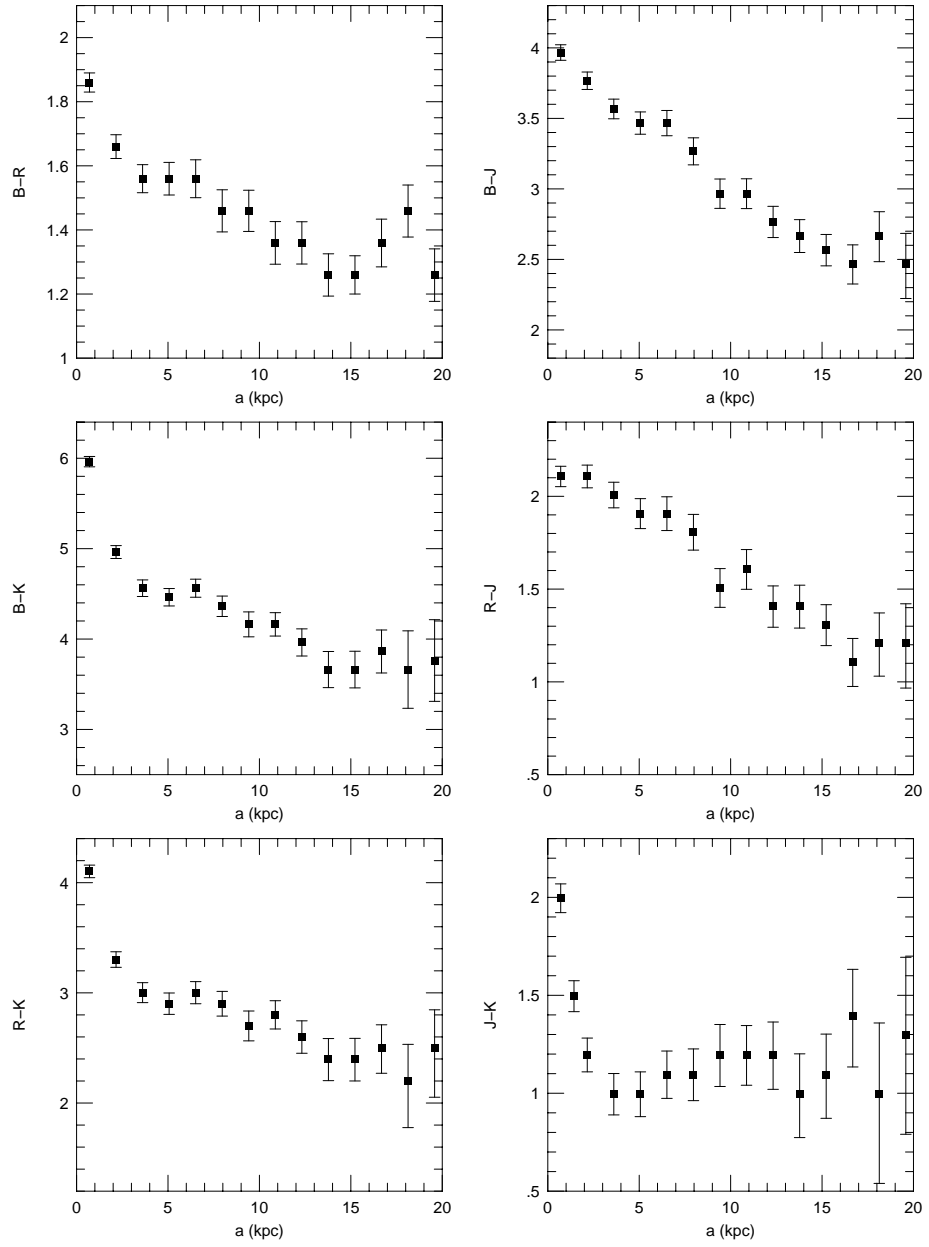


Fig. 6.— Color profiles for 0313-192. The colors have been corrected for galactic extinction. No K-correction has been applied. Notice the highly reddened core relative to the disk colors.

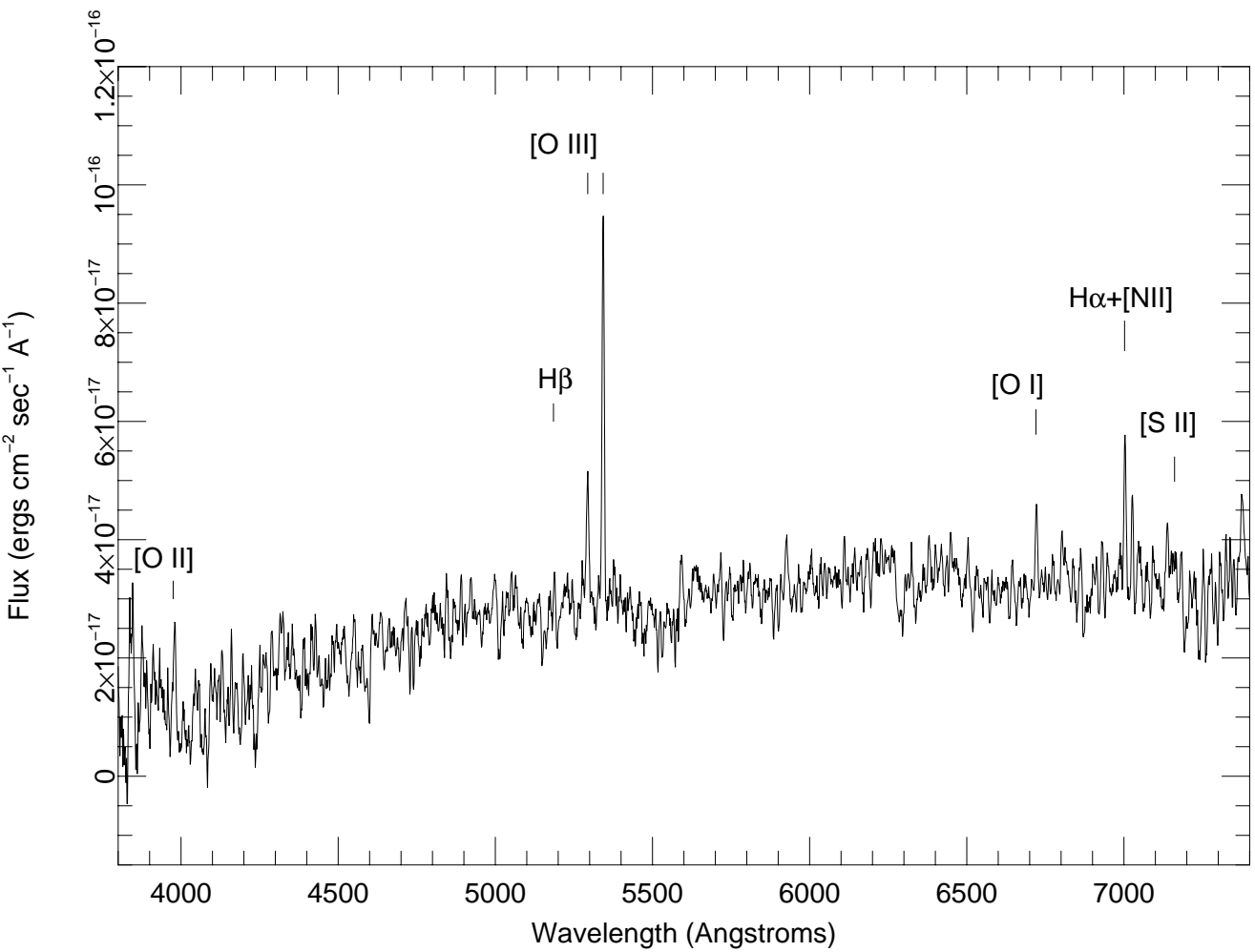


Fig. 7. — The nuclear optical spectrum of 0313-192. The slit orientation was North-South, perpendicular to the disk. The salient features are the AGN-like emission lines, seen through the strong [OIII] and [O I] lines, and relatively weak Balmer emission.

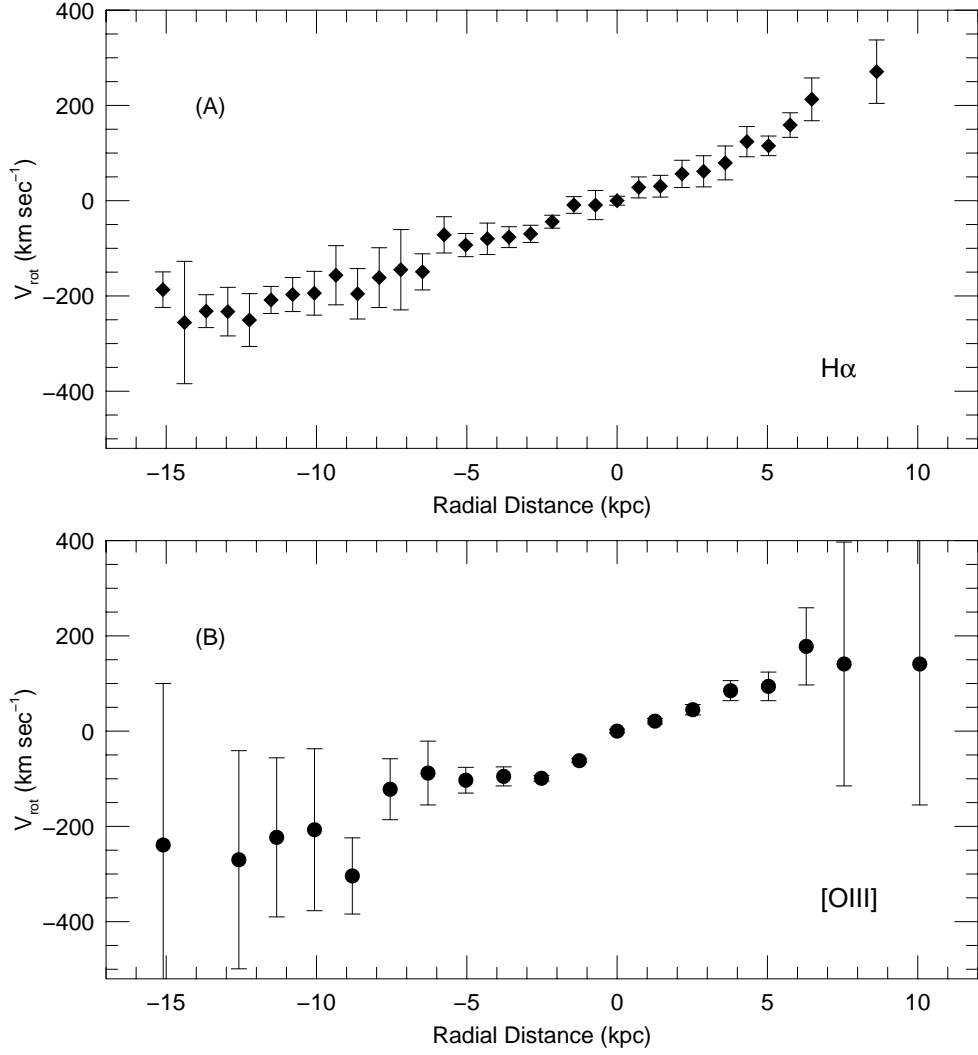


Fig. 8.— The optical rotation curves measured from (a)  $H\alpha + [NII]$ , and (b)  $[OIII]\lambda 4959 + 5007$ . The radial distance is measured relative to the nucleus in kpc, with east defined as positive. We adopt a maximum rotational velocity of  $v_{rot} = 208 \text{ km s}^{-1}$ .